Available online at www.sciencedirect.com
ScienceDirect
Journal of Power Sources 173 (2007) 357–366
JOURNAL OF POWER SOURCES
www.elsevier.com/locate/jpowsour

High temperature electrolyte supported Ni-GDC/YSZ/LSM SOFC operation on two-stage Viking gasifier product gas

Ph. Hofmann [a], A. Schweiger [b], L. Fryda [a], K.D. Panopoulos [a,*], U. Hohenwarter [b], J.D. Bentzen [c], J.P. Ouweltjes [d], J. Ahrenfeldt [e], U. Henriksen [e], E. Kakaras [a]

[a] *Laboratory of Steam Boilers and Thermal Plants, School of Mechanical Engineering, Thermal Engineering Section, National Technical University of Athens, 9 Heroon Polytechniou Avenue, Zografou, 15780 Athens, Greece*
[b] *Graz University of Technology, Institute of Thermal Engineering, Inffeldgasse 25/B, 8010 Graz, Austria*
[c] *COWI A/S, Parallelvej 2, 2800 Kongens Lyngby, Denmark*
[d] *Energy Research Centre of the Netherlands ECN, P.O. Box 1, 1755 ZG Petten, The Netherlands*
[e] *Biomass Gasification Group, Department of Mechanical Engineering, Technical University of Denmark, 2800 Kongens Lyngby, Denmark*

Received 4 December 2006; received in revised form 26 March 2007; accepted 29 April 2007
Available online 5 May 2007

Abstract

This paper presents the results from a 150 h test of a commercial high temperature single planar solid oxide fuel cell (SOFC) operating on wood gas from the Viking two-stage fixed-bed downdraft gasifier, which produces an almost tar-free gas, that was further cleaned for particulates, sulphur and tar traces. The chosen SOFC was electrolyte supported with a nickel/gadolinium-doped cerium oxide (Ni-GDC) anode, known for its carbon deposition resistance. Through humidification the steam to carbon ratio (S/C) was adjusted to 0.5, which results in a thermodynamically carbon free condition at the SOFC operating temperature $T = 850\,^{\circ}C$. The cell operated with a fuel utilisation factor (U_f) around 30% and a current density of 260 mA cm^{-2} resulting in an average power density of 207 mW cm^{-2}. Throughout the duration of the test, only a minor cell overpotential increase of 10 mV was observed. Nevertheless, the *V–j* (voltage–current density) curves on H_2/N_2 before and after the wood gas test proved identical. Extensive SEM/EDS examination of the cell's anode showed that there was neither carbon deposition nor significant shifts in the anode microstructure or contamination when compared to an identical cell tested on H_2/N_2 only.

Keywords: Solid oxide fuel cell; Two-stage gasification; Biomass; Wood gas; Nickel gadolinium-doped ceria oxide

1. Introduction

Small scale efficient combined heat and power (CHP) plants based on biomass gasification coupled with emerging technologies for power production such as micro gas turbines and fuel cells have lately gained increasing attention. For big plants (more than 100 MW thermal) combustion with steam cycle has economic advantages. Smaller scale gasification systems with internal combustion engines are now demonstrated during several thousands of hours to give reasonable electrical efficiencies and limited emissions; however fuel cells have the potential to obtain even higher electric efficiencies, and lower emissions. High temperature fuel cells, such as the SOFC, can utilise the major product gas combustible content (H_2, CO and CH_4) offering increased efficiencies, and high quality thermal energy from the off gases, which can be further used in gas turbines or for system integration and process heating.

Nevertheless the commercialisation of integrated biomass gasification with SOFC, apart from problems associated with each technology separately, largely depends on the degradation impact of the wood gas main species and impurities on SOFC anode materials. Common wood gas impurities are (a) particulates of ash and non-converted char which can cause carbon deposition on SOFC anodes, (b) H_2S which is the most documented impurity for SOFC fuels and reported to be potentially permanently poisonous at levels above 1 ppmv [1], (c) NH_3 is reported to be a highly efficient SOFC fuel without degradation effect [2], (d) HCl and other halides are reported to be poisonous at levels above 1 ppmv [1]. Other biomass product gas impurities, scarcely documented for their effect on SOFC

* Corresponding author. Tel.: +30 210 7721213; fax: +30 210 7723663.
E-mail address: kik@central.ntua.gr (K.D. Panopoulos).

0378-7753/$ – see front matter © 2007 Elsevier B.V. All rights reserved.
doi:10.1016/j.jpowsour.2007.04.073

Nomenclature

A	SOFC active surface area (cm^2)
F	Faraday constant ($6.023 \times 10^{23} \times 1.602 \times 10^{-19}$ C mol^{-1})
ΔG°	Gibbs energy change of the H_2 electrochemical reaction (J mol^{-1})
I	fuel cell current (A)
j	current density (mA cm^{-2})
LHV	anode fuel low heating value (MJ Nm^{-3})
$\dot{n}_c$	cathode molar flow (mol s^{-1})
$\dot{n}_f$	anode fuel molar flow (mol s^{-1})
$\dot{Q}_c$	cathode normal volume flow (N ml min^{-1})
$\dot{Q}_f$	anode fuel normal volume flow (N ml min^{-1})
R	universal gas constant (8.314 J mol^{-1} K^{-1})
$S/C_{1\text{ or }2}$	water steam to carbon species ratio: (1) including CO_2 or (2) excluding
T_{cell}	temperature of the fuel cell (K)
U_f	fuel utilisation factor
U_{O_2}	oxygen utilisation factor
V_{cell}	fuel cell measured voltage (V)
V_N	evaluated Nernst fuel cell potential (V)
x_i	mole fraction of component i

Greek letters

η_{cell}	fuel cell voltage overpotentials (V)
η_{el}	fuel cell electrical efficiency

operation, include (e) aggressive volatile alkali compounds that might escape if high temperature gas cleaning is solely employed and (f) tars, which is a complex mixture of organic compounds mostly of aromatic nature that derive from the biomass pyrolysis products and secondary reactions [3]. The latter could result in carbon deposition on Ni containing anodes, proved by a theoretical study from D. Singh et al. [4] who performed bulk gas thermodynamic equilibrium calculations on different SOFC operating conditions and tar contents. Nevertheless experimental studies are required to obtain a clearer picture on how tars and other product gas species (such as CH_4 and CO) could lead to carbon formation and deposition on SOFC anodes. In the extensively studied conventional steam reforming catalysis a S/C (the molar ratio of steam to carbon) of around 2.5–3 is commonly used to prevent carbon deposition [5]. While operating a SOFC with such high steam content provides safety against carbon deposition, this may create overall system efficiency penalties due to the thermal requirements for steam production. Therefore, carbon deposition resistant anode materials should be used in such applications, where contamination with heavy hydrocarbons might occur. In general, one of the most promising SOFC anode materials to reduce risks of carbon deposition is Ni-GDC; such anodes have operated stably on weakly humidified (∼3% H_2O) methane at 800 °C [6]. GDC is able to oxidise/gasify carbon deposits during or after CH_4 decomposition on a Ni-GDC cermet through its bulk lattice oxygen content, forming CO or CO_2 [7,8].

Most of the experimental works published on this topic so far, investigate the impact of simulated product gas on SOFC performance. S. Baron et al. [9] tested intermediate operating temperature ($T = 650$ °C) Ni-GDC anode SOFCs with various emulated gasification mixtures and found that CO decreased the performance of the cell when compared to H_2 and that CH_4 up to 10% with S/C = 1 resulted in poor power output due to carbon deposition. In a similar work, Ouweltjes et al. [10] tested the effect of simulated product gas at thermodynamically carbon deposition free regions ($T = 850$–920 °C) on Ni-GDC anodes, including H_2S up to 9 ppmv in the anode feed. The latter was found to deactivate the anode for methane reforming but did not affect the hydrogen nor carbon monoxide electrochemical oxidation reactions, while no carbon deposition was observed at S/C as low as 0.8. The effect of even higher H_2S concentrations up to 240 ppmv on planar anode supported SOFC was studied by Hustad et al. [11] who concluded that performance was significantly reduced even at 5 ppmv H_2S but above a concentration of around 10–20 ppm there was only marginal additional cell performance degradation. Suwanwarangkul et al. [12] observed carbon deposition on Ni–CeO_2–YSZ anode surface after operation on different syngas mixtures at 800 °C assuming the Boudouard reaction responsible. However at 900 °C no carbon deposition was observed.

Investigations of high temperature SOFCs running on actual product gas from biomass gasification in an integrated biomass fuel cell (BFC) system are limited. Apart from the present work obtained within the ongoing EU project BioCellUS (Biomass fuel Cell Utility System) [13], Oudhuis et al. have coupled a two-stage gasifier to a downscaled 'state of the art' Sulzer HEXIS stack for a maximum of 48 h [14], showing that the principle works but observing soot formation during fuel heating which negatively influenced the cell performance (reversibly). In [15], the electrochemical performance of low temperature (600 °C) SOFC with Ni-SDC and Ni/Cu-SDC anodes and thin film GDC electrolyte were tested with both humidified hydrogen as well as syngas from biomass gasification, nevertheless very little information is given about the experimental facility such as the gasifier and the gas cleaning apparatus. Carbon deposition was substantially suppressed when employing Ni/Cu in comparison to Ni containing anodes. The addition of Cu however is only applicable to low temperature SOFCs because of its low melting temperature and reduced stability at higher temperatures.

This paper presents the results from a 150 h performance test of a high temperature single planar SOFC with Ni-GDC anode fuelled with almost tar-free wood gas produced from the Viking gasifier developed at the Danish Technical University (DTU). The goal of the experiment was to achieve a steady operation of a commercial SOFC with a very clean wood gas delivered by an existing biomass gasifier and relatively low humidification at S/C = 0.5, but still in the thermodynamic carbon formation free region.

2. Experimental

The details of the experimental setup for testing a planar SOFC fuelled with wood derived gas from the Viking

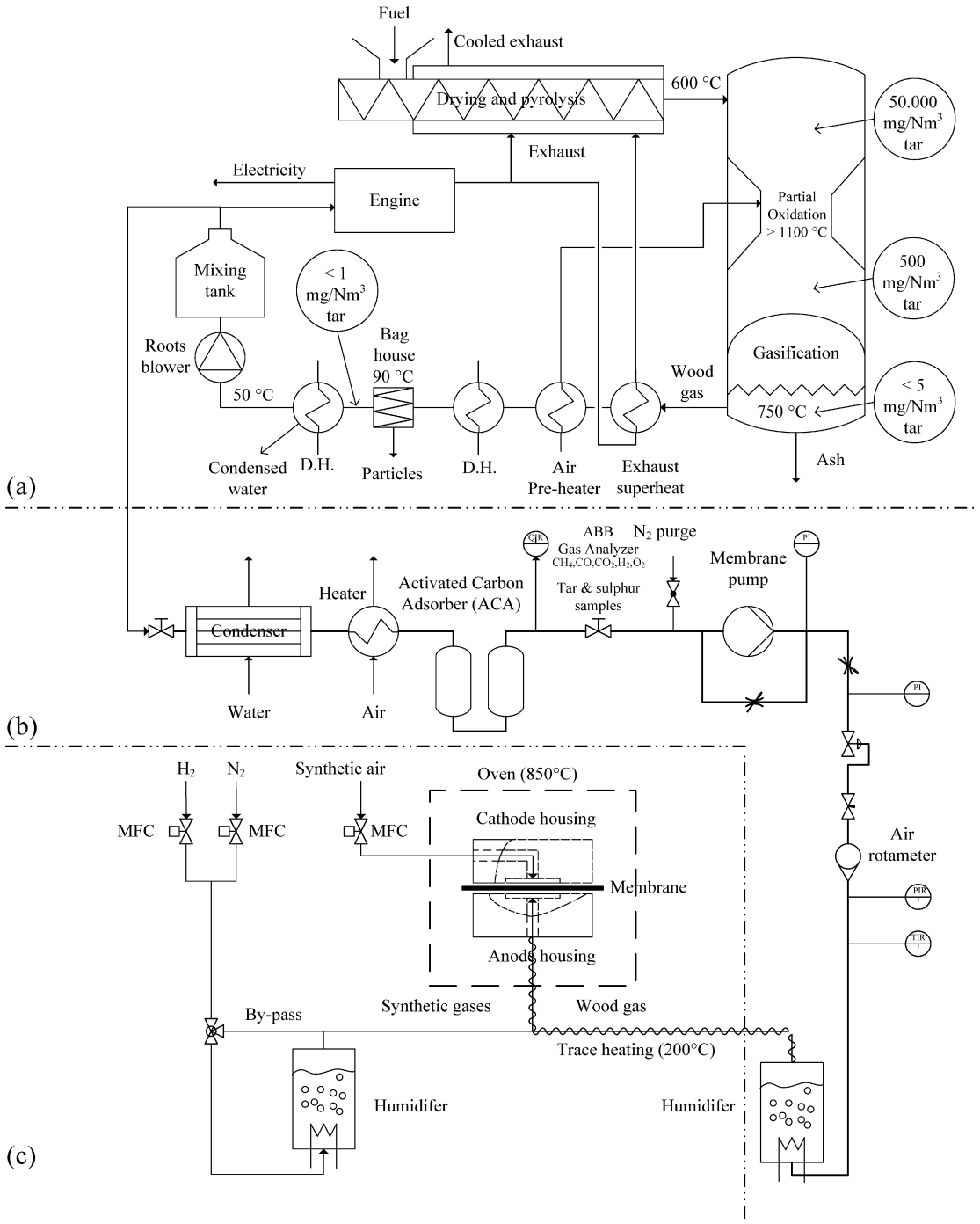

Fig. 1. (a) Two-stage fixed-bed downdraft gasifier "Viking" CHP [17]. (b) Gas cleaning and gas conditioning unit, and (c) SOFC test rig.

two-stage gasifier are shown in Fig. 1 that comprises three sections:

(a) The Viking gasifier combined heat and power (CHP) system converting biomass into an almost tar-free product gas, which is currently fed to a gas engine.
(b) A slip stream from the gas buffer/mixing tank of the CHP unit was further cleaned, conditioned, its composition was analysed and its flow rate towards the SOFC controlled.
(c) The planar SOFC test rig consisting of a single cell setup with current load regulation, cell voltage measurement as well as alternative bottled gas supply and gas humidification.

More detailed descriptions of each section and the experimental procedure followed is given in the following sections.

2.1. Gasifier

A schematic of the existing two-stage fixed-bed downdraft gasifier Viking at the Technical University of Denmark (DTU) is shown in section (a) of Fig. 1. Characteristic operational data

Table 1
Key data for the Viking gasifier CHP plant

Thermal input	68 kW
Fuel	Wood chips of spruce
Moisture content preferred	<45%
Cold gas efficiency	93%
Engine efficiency	32%
Electric efficiency	27%
Overall electric efficiency	25%
Tar level	<1 mg Nm^{-3}
Dust level	<5 mg Nm^{-3}
Operation	Unmanned/unattended
Hours of operation	3500

of this facility are summarised in Table 1. An important feature of this concept is that pyrolysis and gasification take place separately, and in between, pyrolysis products are partially oxidised by introducing preheated air which results in increasing temperature to around 1100 °C. Consequently the tar content from the pyrolysis gaseous products is significantly reduced by partial oxidation and thermal decomposition. The hot gases' sensible heat provides the required thermal energy for the endothermic char gasification. The wood gas tar content is significantly further reduced when passing through the char bed. The resulting tar load of the produced wood gas is less than 1 mg Nm^{-3} [16]. A more detailed description of the Viking gasifier concept is given by Henriksen et al. [17].

In the existing CHP facility, the wood gas is cooled down to 90 °C by passing through several heat exchangers which deliver heat for integration and heating purposes. At this temperature any soot particles are removed dry in a bag house filter, while further cooling condenses out most of the water content and the dry-cool wood gas is finally fed to a gas engine coupled to a generator. The gas engine is an integrated part of the whole gasification plant, since exhaust gases are utilised for drying and pyrolysis of the biomass in the gasification system, but eventually could be replaced by a SOFC stack.

2.2. Gas conditioning and analytical measurements

The SOFC was fuelled from a slipstream out of the buffer/mixing tank of the CHP unit. Fig. 1(b) shows the process steps that the wood gas underwent prior to its feeding to the SOFC. Two adsorbing materials were used consecutively in an activated carbon adsorber (ACA) unit: Norit ROZ3 for sulphur removal, and Norit RB3 for removal of polycyclic aromatic hydrocarbons (PAHs). For protecting the activated carbon against deactivation by water condensation the gas moisture level was controlled by a condenser/heater unit before the ACA. A gas sampling slipstream for analyses was drawn after the ACA. A membrane pump and mechanical pressure regulator supplied a pressure pulse free wood gas flow through the humidifier to the SOFC anode side.

The permanent gas composition was measured on-line with an ABB^{TM} analyser incorporating NDIR detector for CO, CH_4, and CO_2, paramagnetic detector for O_2 and a TCD for the H_2 content. Finally N_2 content was evaluated by difference. The wood gas flow to the SOFC was adjusted by a commercial gas rotameter with an integrated needle valve and was calculated taking into account the measured main gas composition, rotameter scale indication and outlet temperature and pressure. The moisture level to reach the desired S/C was achieved by passing the wood gas through a temperature controlled humidifier with demineralised water. The connection between humidifier and SOFC fuel inlet was trace heated (200 °C) to avoid water condensation and to preheat the flow before it reached the SOFC test rig.

To confirm the wood gas tar load elimination during the operation, a solid phase adsorption (SPA) sampling was taken after the ACA and analysed with gas chromatography/mass spectrometry (GC/MS) using stable isotopes as the internal standard. Gas samples from the same sampling point were also analysed for sulphur trace compounds (H_2S, COS, CS_2 and SO_2) using gas chromatography (GC) equipped with a pulsed flame photometric detector (PFPD). A DRÄGER-Tube system (tube type Hydrosulphide 2/a) with a H_2S detection limit from 2 to 20 ppm was used to cross-check the GC measurements.

2.3. SOFC

2.3.1. SOFC membrane

The experiment was performed with a circular shaped planar electrolyte-supported SOFC membrane manufactured by InDEC B.V., consisting of a nickel/gadolinium-doped cerium oxide (Ni/GDC) anode, yttrium stabilised zirconium oxide (YSZ) electrolyte and a strontium doped lanthanium manganite (LSM) cathode, with a diameter of 120 mm and an active surface area of $A = 100\,cm^2$. The cell's main features are summarised in Table 2.

2.3.2. Test rig

The mobile SOFC single-cell test rig together with its peripheral equipment is shown in Fig. 1(c). A detailed description can be found in [10]. The seal-less ceramic cell housing consists of Al_2O_3 flanges with channels for gas distribution, to which the current collectors, i.e. platinum gauze for the cathode and nickel gauze for the anode, were spot-welded. Depleted anode and cathode gases burn outside the cell; thus gas measurement of the anode outlet gases was not possible. The cell housing together with the anode and cathode gas tubes were placed in a temperature-controlled oven. A thermocouple measures the tem-

Table 2
Planar SOFC material characteristics

Parameter	Thickness (μm)	Layer	Composition
Anode	40	Current collecting, functional, contact	Ni, Ni and $Gd_{0.1}Ce_{0.9}O_2$ (10GDC), $Gd_{0.4}Ce_{0.6}O_2$
Electrolyte	90		$Y_{0.06}Zr_{0.94}O_2$ (3YSZ)
Cathode	40	Functional, current collecting	$La_{0.75}Sr_{0.2}MnO_3$ (LSM) and $Y_{0.16}Zr_{0.84}O_2$ (8YSZ), $La_{0.75}Sr_{0.2}MnO_3$ (LSM)

perature at the centre of the cell where anode and cathode gases enter from where they radially spread along the membrane. The *V–j* characteristics were measured with a variable electronic load (PLZ 664WA Kikusui Electronics Corp., Japan) which is supported by an additional power supply unit (SM120-25D Delta Elektronica, Zierikzee, Netherlands) in order to compensate for the low cell voltage. All collected signals were logged in a data acquisition system.

A mixture of H_2 and N_2 from bottled gases was used for the conditioning of the cell and allowing wood gas independent operation. In that case, flows were adjusted with Bronkhorst mass flow controllers while the level of humidification was again set by passing the gas mixture through a temperature controlled water bubbler, which could also be by-passed. The anode feed gas line consisted of trace-heated steel and ceramic tubing which was connected to the bottom of the ceramic cell housing.

2.3.3. Experimental procedure

The rate of heating and cooling of the oven containing the cell was restricted to $40\,^{\circ}C\,h^{-1}$ in order to prevent thermal stresses in the ceramic flanges of the cell housing. The procedure for heating-up, reduction and conditioning of the cell prior to wood gas operation as well as the cool-down procedure with the respective anode and cathode flows is summarised as follows:

$$25\,^{\circ}C \xrightarrow[500\,N\,ml\,min^{-1}\ syn.\ air]{500\,N\,ml\,min^{-1}\ N_2} 750\,^{\circ}C\ (\text{cell reduction} \sim 45\,\text{min})$$

$$\xrightarrow[500\,N\,ml\,min^{-1}\ syn.\ air]{0\text{–}500\,N\,ml\,min^{-1}\ H_2} 750\,^{\circ}C \xrightarrow[1500\,N\,ml\,min^{-1}\ syn.\ air]{500\,N\,ml\,min^{-1}\ H_2} 850\,^{\circ}C(>1\,h)$$

$$\xrightarrow[2000\,N\,ml\,min^{-1}\ syn.\ air]{350/450\,N\,ml\,min^{-1}\ H_2/N_2} V\text{–}j\ \text{curve}$$

$$\rightarrow \text{wood gas operation for } 150\,h$$

$$\rightarrow (1\,h) \xrightarrow[2000\,N\,ml\,min^{-1}\ syn.\ air]{350/450\,N\,ml\,min^{-1}\ H_2/N_2} V\text{–}j\ \text{curve}$$

$$\xrightarrow[500\,N\,ml\,min^{-1}\ syn.\ air]{40/760\,N\,ml\,min^{-1}\ H_2/N_2} 25\,^{\circ}C$$

The reference gas mixture for *V–j* curves consisted of $350\,N\,ml\,min^{-1}$ H_2 together with $450\,N\,ml\,min^{-1}$ N_2 (both bottled) on the anode side and $2000\,N\,ml\,min^{-1}$ synthetic air on the cathode side. All anode gas mixtures outside wood gas operation were humidified at room temperature during the described procedure (approx. 3 vol.% H_2O). A slight reducing atmosphere was sustained on the anode side during the cool-down procedure to prevent the re-oxidation of the nickel. Bottled pure gases of laboratory standard 5.0 were used for N_2, H_2 and synthetic air (80 vol.% N_2, 20 vol.% O_2).

After switching the cell to wood gas operation, the first 1.5 h were operated at open-circuit voltage (OCV) in order to allow the cell to adapt to the new feed gas composition. By taking the first *V–j* curve on wood gas, the current load was increased stepwise to the operational current $I = 26$ A, i.e. a current density of $260\,mA\,cm^{-2}$. Intermediate *V–j* curves were measured during wood gas operation, while the final *V–j* curve on wood gas before the end of the 150 h test resulted from the step-wise decrease of the current density to OCV.

2.3.4. Post-experimental analysis of SOFC membranes

The microstructure of the SOFC anode was characterised using an analytical scanning electron microscope (SEM). Extensive examination with energy dispersive spectrometry (EDS) was employed to determine any carbon deposition on the anode structure. For comparison reason an identical SOFC membrane was solely used on a reference H_2/N_2 $350/450\,N\,ml\,min^{-1}$ anode mixture humidified at room temperature, and cathode synthetic air flow of $2000\,N\,ml\,min^{-1}$. Both cells were cross examined with SEM to identify possible differences.

3. Results and discussion

Stable operation of the gasifier was obtained throughout the 150 test hours connected to the SOFC. There is no indication of an up/downwards trend of specific gas compounds, however periodic fluctuations of the gas composition could be observed related to the operation of the fixed bed gasifier, as shown in Fig. 2. Twice during the test period the gasifier shut down automatically due to serious channel formation in the char bed in the gasification reactor. At these two incidents the gasifier was put back in operation after 26 and 11 min, respectively. Nevertheless, the SOFC was kept on wood gas supplied from the mixing tank. Some short oxygen peaks in the order of 3% could be observed resulting from these shutdowns as well as from some other minor interruptions. It can be assumed that these peaks did not cause oxidation of the anode since this small amount of O_2 would quickly react with hydrogen and carbon monoxide once the wood gas reached the high temperature oven (before it reached the SOFC).

Table 3 includes the average gas species concentrations as well as average derived characteristics of the wood gas such as

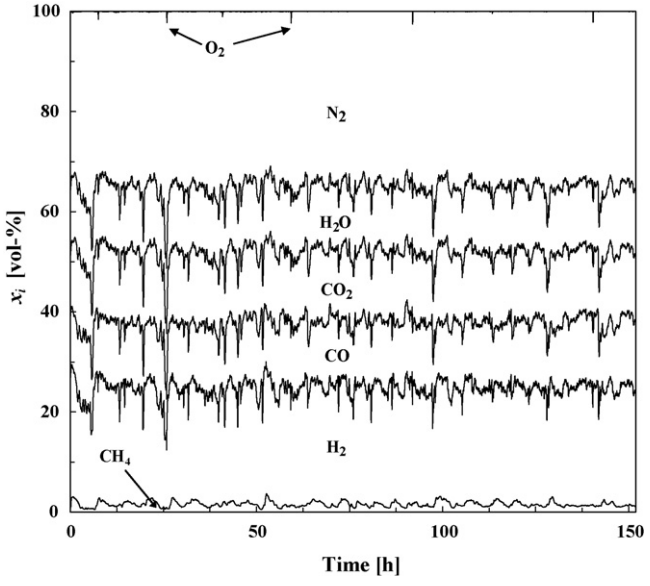

Fig. 2. Wood gas composition after re-humidification (cumulative) vs. time.

Table 3
Conditioned wood gas and SOFC operation characteristics

Parameter	Unit	Equation		Average	S.D.
Gas composition					
x_{H_2}				23.10	1.76
x_{CO}				12.93	1.09
x_{CH_4}	vol.%			1.57	0.55
x_{CO_2}				14.08	0.82
x_{N_2}				35.30	0.10
x_{H_2O}				13.00	–
Measured SOFC parameters					
V_{cell}	mV			797	6
j	mA cm^{-2}			260	–
T_{cell}	°C			850	2
$\dot{Q}_f$	N ml min^{-1}			1132	–
$\dot{Q}_c$	N ml min^{-1}			2000	–
Derived parameters					
LHV	MJ Nm^{-3}			4.69	0.27
S/C$_1$	–	$S/C_1 = \frac{x_{H_2O}}{x_{CH_4} + x_{CO} + x_{CO_2}}$	(1)	0.46	0.02
S/C$_2$	–	$S/C_2 = \frac{x_{H_2O}}{x_{CH_4} + x_{CO}}$	(2)	0.90	0.06
U_f	%	$U_f = \frac{I}{2F\dot{n}_f(x_{H_2} + x_{CO} + 4x_{CH_4})}$	(3)	30.36	2.02
U_{O_2}	%	$U_{O_2} = \frac{I}{4F\dot{n}_c x_{O_2}}$	(4)	23	–
η_{el}	%	$\eta_{el} = \frac{V_{cell} I}{LHV \cdot \dot{V}_f}$	(5)	23.57	1.40

its lower heating value (LHV) and steam to carbon ratio (S/C). Their progress with time is shown in Fig. 3: the wood gas LHV is quite steady between 4 and 5 MJ Nm^{-3} during most of the testing period with a slight amelioration towards the end. The steam to carbon ratio (S/C) after re-humidification of the wood gas was around 0.46 or 0.90, depending on its definition given by Eq. (1) or (2), shown in Table 3.

The C–H–O ternary diagram of Fig. 4 displays the boundary line for solid carbon formation at 850 °C predicted by thermodynamic equilibrium calculations. Two average anodic gas composition points are plotted: one point represents SOFC operation at OCV, while the other point represents the operation on current (I = 26 A), which in the form of O^{2-} runs through the membrane. In the latter case, the oxygen content of the anode gas mixture is increased by (I/2F) mol O^{2-} s^{-1}. It is clear that at the SOFC operational temperature of 850 °C the tests have been carried out in a thermodynamic carbon deposition free environment. The risk of carbon deposition was further reduced since the wood gas was almost tar free. The SPA sampling and analysis results,

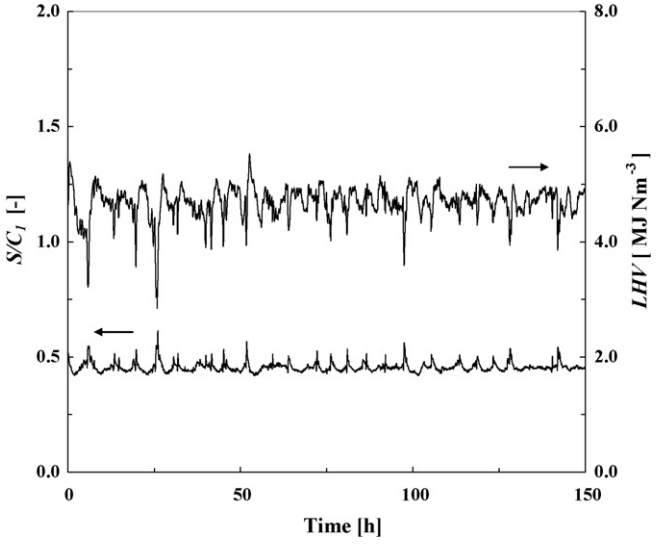

Fig. 3. Anode feed gas lower heating value (LHV) and S/C$_1$ ratio vs. time.

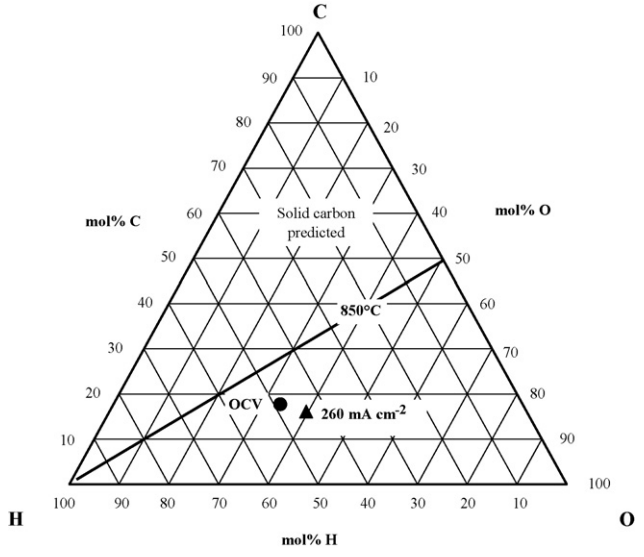

Fig. 4. C–H–O ternary diagram: thermodynamic equilibrium prediction of solid carbon for a gas composition above the line for 850 °C.

Table 4
Results from the GC/MS analysis of the SPA tar sampling

Compound	Concentration (mg Nm^{-3})
Phenol	0.00
Naphthalene	0.17
Phenanthrene	0.00
Anthracene	0.00
Fluoranthene	0.00
Chrysene	0.00
Pyrene	0.00

Table 5
Sulphur analysis results

Sample	Concentration (ppmv)			
	H_2S	COS	CS_2	SO_2
1	0	0.28	0	0
2	0	0.17	0	0

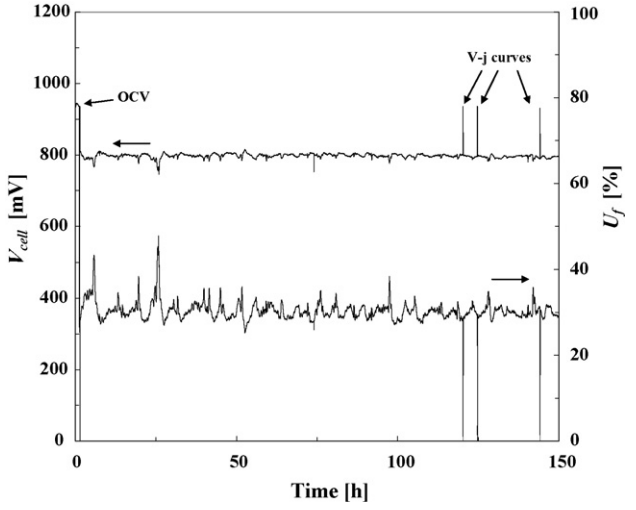

Fig. 5. Cell voltage and fuel utilisation (U_f) vs. time.

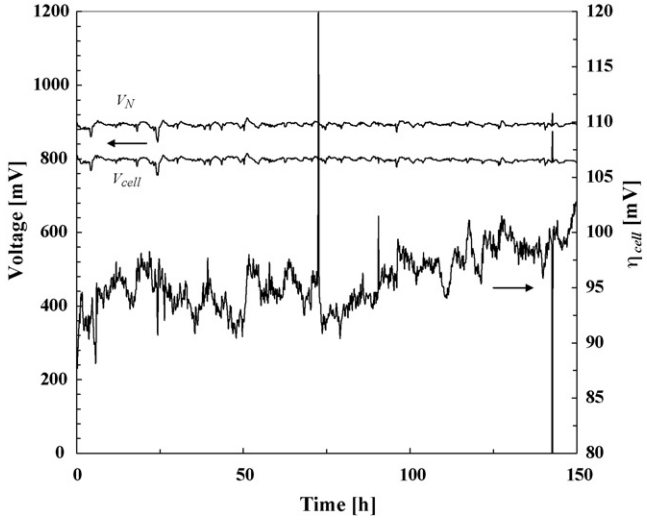

Fig. 6. Nernst potential, cell voltage and difference (overpotentials) vs. time for operation on 260 mA cm^{-2} current density load.

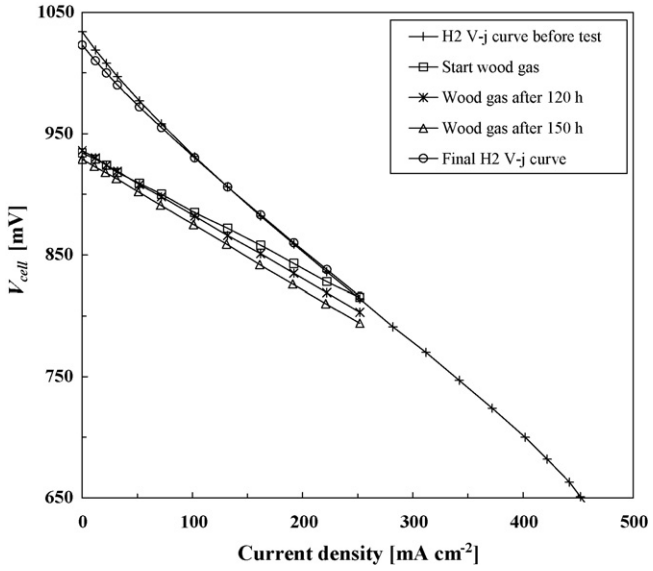

Fig. 7. *V–j* curves on H_2 before wood gas, onset and during wood gas operation, and on H_2 after wood gas operation.

given in Table 4, proved that the conditioned wood gas contained negligible amount of tars, namely only 0.17 mg Nm^{-3} naphthalene. Furthermore, Table 5 shows the results from the analysis for sulphur compounds: there was no detectable H_2S contamination and a close to the detection limit COS concentration.

The average and standard deviation of the most important results and characteristics of the SOFC operation on wood gas are also presented in Table 3. The wood gas composition was fluctuating; therefore cell voltage was not entirely flat with time but remained around 800 mV. Fig. 5 presents the complete course of the measured cell voltage V_{cell} and fuel utilisation U_f over the 150 h of SOFC operation on wood gas from the Viking gasifier. After running approx. 1.5 h at open-circuit voltage (OCV) on wood gas operation, the SOFC was set to a constant current load of 260 mA cm^{-2}. There was no significant voltage decrease

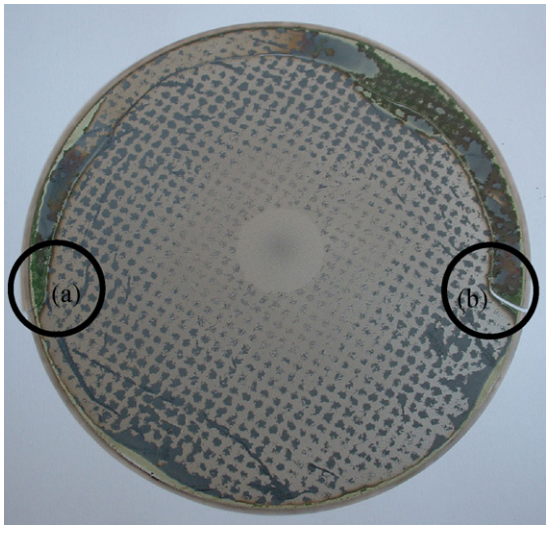

Fig. 8. Photo of anode side after 150 h of operation on wood gas: the two cracks occurred at (a) and (b).

within this test period which would indicate any degradation of cell performance.

The positive voltage peaks in Fig. 5 resulted from *V–j* curve measurements while the negative were due to periodical switching to a new synthetic air gas bottle that interrupted the cathode flow for some seconds. The fuel utilisation U_f was evaluated with Eq. (3), where $\dot{n}_f$ is the anode mole flow, taking into account that CO can produce an extra H_2 through the water gas shift (WGS) reaction, while CH_4 can produce four additional H_2 through its reforming and WGS of produced CO. Finally the extent of electrochemical reactions was determined by the drawn current *I*. The U_f was deliberately kept at a moderate level of around 30%, to avoid risk of anode oxidation since the wood gas composition and flow was fluctuating and the seal-less anode could allow back flow/diffusion of air.

With a fluctuating wood gas composition it is difficult to attribute small changes of cell voltage over time to degradation of cell performance since changes of up to ±50 mV could be related to gas composition fluctuations. A more indicative way to investigate any changes in cell performance over the duration of experiment, is the evaluation of the cell overpotentials, η_{cell}, by partially filtering out the influence of the fluctuation of available fuel (i.e. H_2, CO and CH_4) on cell voltage. That was done by comparing the measured cell voltage (V_{cell}) with the Nernst voltage (V_N) given by Eq. (6) and calculated under the assumptions that only H_2 is the active compound in the electrochemical reaction, and that the WGS reaction and the methane reforming reaction reach thermodynamic equilibrium at the exit of cell:

$$V_N = \frac{-\Delta G^o}{2F} + \frac{RT_{cell}}{2F} \ln\left(\frac{x_{H_2}\sqrt{x_{O_2}}}{x_{H_2O}}\right) \quad (6)$$

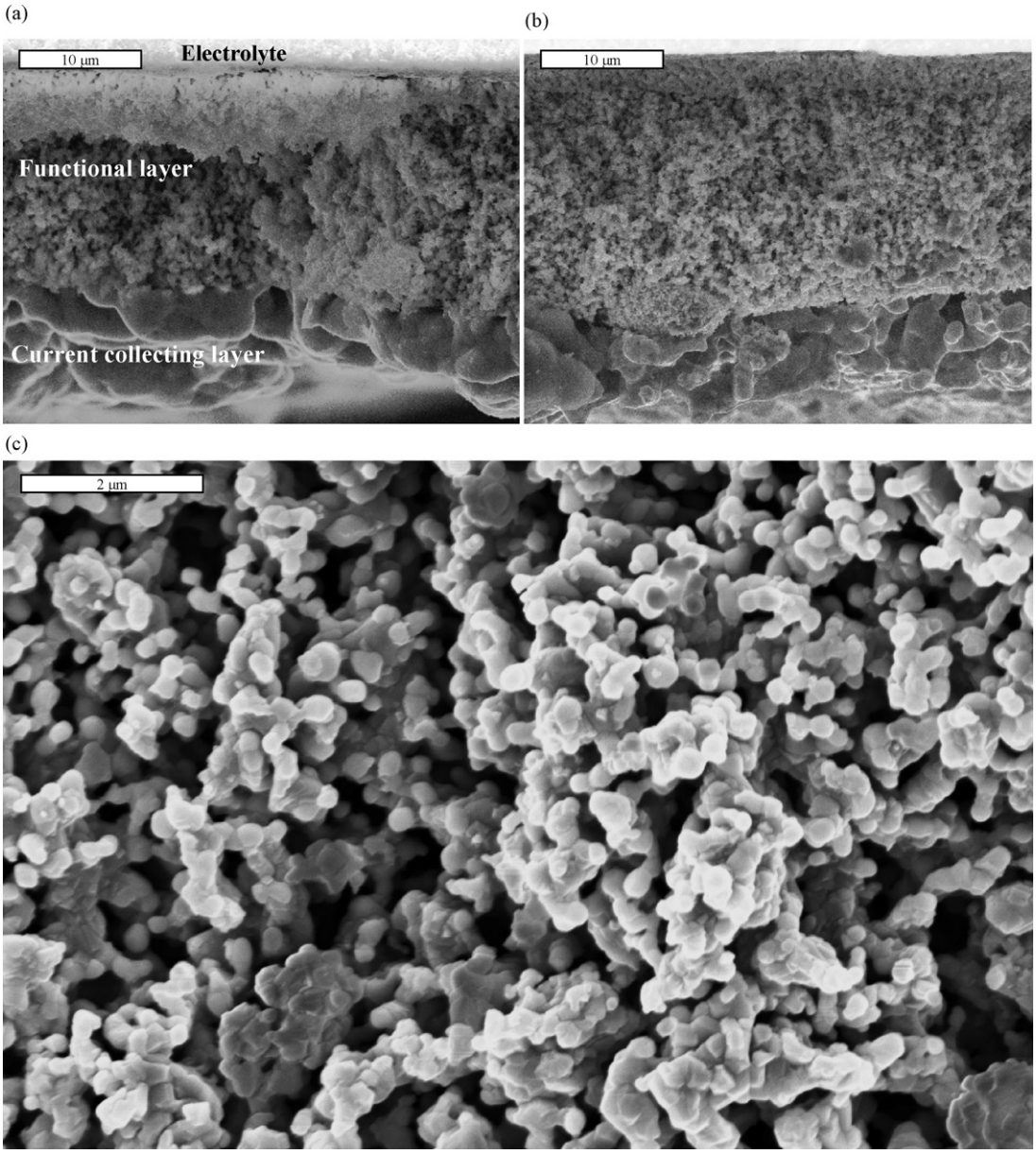

Fig. 9. SE micrographs of the SOFC anode sides (a) after the 150 h operation on wood gas, compared with (b) an identical SOFC cell operated for 1.5 h on H_2, and (c) detailed SE micrograph of the functional layer of the SOFC operated on wood gas.

The mole fractions of H_2, H_2O and O_2 used in Eq. (6) were the values evaluated at the cell's exit, assuming that the total pressure on both anode and cathode side is equal to the standard 1 atm. For the duration of the experiment V, V_N, and overpotentials η_{cell} are shown with time in Fig. 6, from which a negligible increase of approx. 10 mV in η_{cell} can be observed at the end of the 150 h test run on wood gas. This is very difficult to attribute to degradation effects because of the existing dependence of activation overpotentials with the gas composition.

Several *V–j* curves measured during wood gas operation as well as before and after that, with the reference H_2/N_2 mixture (humidified at room temperature), are shown in Fig. 7. The curves obtained on H_2/N_2 show an 11 mV drop at OCV after 150 h on wood gas operation. At higher current densities the *V–j* curves coincide, suggesting no degradation whatsoever. The *V–j* curves obtained during wood gas operation allow little comparison since gas composition and anode flow were fluctuating throughout the course of the test run.

Fig. 8 shows a photograph of the planar membrane after its operation on wood gas. After dismantling the test rig, two cracks at the outer rim of the cell were observed, adjacent to oxidised nickel zones. Air crossover through these cracks oxidised locally the Ni containing anode but apparently this did not have any serious effect on the overall operation of the SOFC, since the *V–j* curves before and after the test proved identical (Fig. 7) throughout a wide range of current load.

The SEM analysis of the wood gas operated SOFC focused on the identification of any chemical or physical shift of the anode side compared to an identical membrane that was operated on pure H_2/N_2 mixture. In Fig. 9(a), a SE micrograph of a cross section from the wood gas operated cell is shown; its nickel current collecting layer is more sintered and nickel particles agglomerated to larger complexes compared to the H_2/N_2 operated reference cell, from which a SE micrograph is shown in Fig. 9(b). Nickel sinters gradually with time and this layer shrinks. Sintering was given more time in the case of wood gas operated cell (150 h) compared to H_2/N_2 cell (1 h), which explains the relative thickness difference (5–10 μm). Apart from allowing better current collection, the nickel layer serves to prevent nickel migration and evaporation from the anode functional layer. Such nickel layer shrinking is not affecting the SOFC operation and cannot be attributed to any wood gas parameter. EDS mapping showed qualitatively the expected nickel distribution within the anode functional layer. Its porosity, as shown in Fig. 9(c), has not been affected. Elemental dot mapping with EDS on cross sections of the wood gas operated cell did neither reveal any carbon deposits nor contamination from sulphur compounds.

4. Conclusions

Most of the available works published up to now on combinations of SOFC and biomass gasification were based on simulated syngas from bottles. In the present work, a planar high temperature Ni-GDC/YSZ/LSM SOFC was operated successfully for 150 h on wood gas from an existing two-stage biomass gasifier. The wood gas pre-treatment included scavenging of sulphur and tar species as well as moderate humidification to achieve a S/C = 0.5. The experimental procedure, which was explained in detail, strengthens the purpose of proving that the technological concept of feeding gas derived from a biomass gasifier into a SOFC is feasible. The "Viking" two-stage gasifier and the applied gas treatment were proven to be efficient in preventing any tar-derived carbon deposition; Ni-GDC anode coped with the remaining traces of contaminants and was not affected negatively (SEM/EDS showed neither carbon deposition or sulphur contamination nor any change in the anode microstructure). The SOFC voltage performance was sustained throughout the duration of the experiment and the minor overpotential increase at the end of the test cannot be attributed to degradation. It has to be noted that the test was performed with a commercial SOFC and a commercial gasifier. The wood gas had inherent composition fluctuations, but this did not have any effect on the successful SOFC operation. In order to assess the adaptability of SOFC technology with biomass gasification technology in less favourable conditions, future efforts should include longer endurance tests at higher fuel utilisation factors, with clean product gas (as received) as well as tests on product gas from gasifiers with higher tar and contaminant species content to assess their impact on different anodes.

Acknowledgement

The investigations were supported by the European Commission within the Sixth Framework Program (STREP BioCellus, Biomass Fuel Cell Utility System, Contract No. 502759).

References

[1] EG & G Services Parsons Inc., Science Applications International Corporation, Fuel Cell Handbook, 5th ed., DOE/NETL-2000/1110, National Energy Technology Laboratory, Morgantown, WV, 2000.
[2] N. Dekker, G. Rietveld, Highly efficient conversion of ammonia into electricity by solid oxide fuel cells, in: Proceedings of the Sixth European Solid Oxide Fuel Cell Forum, Lucerne, Switzerland, 28 June–2 July, 2004.
[3] T.A. Milne, N. Abatzoglou, R.J. Evans, Biomass Gasifier 'Tars': Their Nature, Formation and Conversion, NREL Technical Report (NREL/TP-570-25357), 1998.
[4] D. Singh, E. Hernández-Pacheco, Ph.N. Hutton, N. Patel, M.D. Mann, J. Power Sources 142 (2005) 194–199.
[5] R.M. Ormerod, in: S.C. Singhal, K. Kendall (Eds.), High Temperature Solid Oxide Fuel Cells: Fundamentals, Design and Applications, Elsevier Advanced Technology, Oxford, 2003, pp. 333–362.
[6] W. Wang, S.P. Jiang, A.I. Yoong Tok, L. Luo, J. Power Sources 159 (2006) 68–72.
[7] T.-J. Huang, Ch.-H. Wang, Methane decomposition and self de-coking over gadolinia-doped ceria-supported Ni catalysts, Chem. Eng. J. 132 (2007) 97–103.
[8] T.-J. Huang, Ch.-H. Wang, J. Power Sources 163 (2006) 309–315.
[9] S. Baron, N. Brandon, A. Atkinson, B. Steele, R. Rudkin, J. Power Sources 126 (2004) 58–66.
[10] J.P. Ouweltjes, P.V. Aravind, N. Woudstra, G. Rietveld, Biosyngas utilization in solid oxide fuel cells with Ni/GDC anodes, in: Proceedings of the First European Fuel Cell Technology & Applications Conference, Rome, Italy, December 14–16, 2005.
[11] J.E. Hustad, Ø. Skreiberg, T. Slungaard, A. Norheim, O.K. Sønju, H. Hofbauer, R. Rauch, A. Grausam, A. Vik, J. Byrknes, BIOSOFC—technology development for integrated SOFC, biomass gasification and high temperature gas cleaning, in: Proceedings of the Second World Conference

and Technology Exhibition on Biomass for Energy, Industry and Climate Protection, Rome, Italy, 10–14 May, 2004.
[12] R. Suwanwarangkul, E. Croiset, E. Entchev, S. Charojrochkul, M.D. Pritzker, M.W. Fowler, P.L. Douglas, S. Chewathanakup, H. Mahaudom, J. Power Sources 161 (2006) 308–322.
[13] BioCellUS EU project web site: http://www.biocellus.com, http://www.biocellus.de, http://www.biocellus.net.
[14] A.B.J. Oudhuis, A. Bos, J.P. Ouweltjes, G. Rietveld, A.B. van der Giesen, High efficiency electricity and products from biomass and waste; experimental results and proof of principle of staged gasification and fuel cells, in: Proceedings of the Second World Conference and Technology Exhibition on Biomass for Energy, Industry and Climate Protection, Rome, Italy, 10–14 May, 2004.
[15] Z. Xie, Ch. Xia, M. Zhang, W. Zhua, H. Wang, J. Power Sources 161 (2006) 1056–1061.
[16] J. Ahrenfeldt, U. Henriksen, T.K. Jensen, B. Gøbel, L. Wiese, A. Kather, H. Egsgaard, Energy Fuels 20 (2006) 2672–2680.
[17] U. Henriksen, J. Ahrenfeldt, T.K. Jensen, B. Gøbel, C. Hindsgaul, L.H. Sørensen, Energy 31 (2006) 1542–1553.